DEVELOPMENT OF NONDESTRUCTIVE RESIDUAL STRESS PROFILE MEASUREMENT METHODS – THE INTEGRAL METHOD

D. J. Hornbach, P.S. Prevéy[1] and Mark Blodgett[2]

[1]Lambda Research, 5521 Fair Lane, Cincinnati, OH 45227
[2]AFRL/MLLP, WPAFB, OH 45433

ABSTRACT. A modified Integral Method was investigated as a means to nondestructively measure the subsurface residual stress distribution. The technique has been demonstrated to be feasible in aluminum alloys by comparison to established destructive measurement methods.

In the current effort a thorough study of higher energy radiations was conducted to obtain deeper penetrating radiations on titanium and nickel base alloys. Higher energy radiation used in conjunction with the modified Integral Method would provide nondestructive subsurface residual stress measurement in components composed of these alloys.

INTRODUCTION

Several previous studies [1-8] have been directed at developing nondestructive residual stress measurement x-ray diffraction (NRSM XRD) methods of recovering the underlying residual stress distribution from measured non-linear lattice spacing vs. $\sin^2_\psi$ data. Work prior to 1989 is reviewed by Eigenmann, Scholtes and Macherauch.[9] Attempts have been made to estimate both high stress gradients and shear components acting normal to the surface through the depth of penetration of the x-ray beam. All such methods assume some functional form to describe the subsurface strain (or stress) distribution, and seek to find the form of that function which best describes the observed attenuation weighted integral of lattice spacing with depth.

An integral method capable of recovering a generalized approximation of the stress as a function of depth has been described by Wern and Suominen.[10] The method of analysis can be applied to strain data obtained by x-ray diffraction or mechanical means, such as center hole drilling.[11] The Wern method is a means of nondestructive determination of the full triaxial state of stress within the depth of the x-ray penetration, allowing for both a full stress tensor and variation in all of the stress components with depth. Published results[10] show that the necessary equilibrium condition (σ_{33} = 0 at the surface) is achieved in the preliminary tests, even though this condition is not required by the method of solution. The method does not depend upon lattice spacing measurements at extremely small grazing angles, minimizing defocusing errors in peak location, error due to surface roughness, and the difficulties of the LaPlace transform solution method.

The Integral Method was proposed for NRSM in nickel and titanium alloy turbine engine components. It provides a stable solution of the subsurface residual stress profile, and a modified version of the method has been successfully applied in XRD measurements in shot peened and machined 7050-T6 aluminum alloys and ceramics.[12] The method is based upon approximating the unknown z-profile of strain, $\varepsilon(z)$, shown in Equation 1, using Fourier trigonometric series expansion. No prior knowledge of the residual stress distributions is required; the stress distribution is not forced to follow a linear pattern. Standard XRD equipment can be used to collect the data.

The average measured strain profile can be expressed as a function of τ where D is the information depth defined by the penetration of the diffracted x-rays and z is the depth below the surface of the specimen.

Proceedings of the Review of progress in Quantitative Nondestructive Evaluation, Vol. 24
Editors: D.O. Thompson and D.E. Chimenti
July 25-30, 2004, Golden, CO

$$\langle \varepsilon_{\Phi\Psi} \rangle(\tau) = \frac{\int_0^D e^{-\frac{Z}{\tau}} \varepsilon(z) dz}{\int_0^D e^{-\frac{Z}{\tau}} dz} \quad (1)$$

The equation of x-ray strain determination is shown as[10]

$$\langle \varepsilon \rangle_{\Phi\Psi} = \frac{\langle d_{\Phi\Psi} \rangle - d_0}{d_o} = A(\tau) \begin{bmatrix} (\varepsilon_{11}(z)\cos^2\Phi + \varepsilon_{12}(z)\sin 2\Phi + \varepsilon_{22}(z)\sin^2\Phi)\sin^2\Psi \\ +(\varepsilon_{13}(z)\cos\Phi + \varepsilon_{23}(z)\sin\Phi)\sin 2\Psi \\ +\varepsilon_{33}(z)\cos^2\Psi \end{bmatrix} \quad (2)$$

where $A(\tau)$ is the integral operator in Equation 1 and Φ and ψ are the angles that define the direction of strain measurement in the sample coordinate system.

The Integral Method has been demonstrated at Lambda Research using Cu and Cr Kα characteristic radiations as a means of determining the surface and near surface residual stress gradient nondestructively. A 7050-T6 aluminum alloy was chosen deliberately for the method development effort due to the range of penetrations easily achievable with available x-ray tubes.[12] Coupons were mechanically polished or shot peened to produce shallow and deep compression, respectively. A third sample was electrically discharge machined (EDM) to produce surface and near surface tension.

The results of the integral method for the shot peened and EDM specimen are plotted with the conventional layer removal results for the 7050-T6 aluminum samples to a depth of 0.0012 in. in Figures 1 and 2, respectively. Measurements obtained with both Cr and relatively deeper penetrating Cu Kα radiations are included. The results of the integral and layer removal methods are considered to be in reasonable agreement within the penetration depth of each respective radiation.

The relative depth of penetration in the 7050-T6 aluminum was considerably greater than the proposed IN100 and Ti base alloys of interest in the present application. Higher energy radiations are required to provide adequate penetration on the order of 0.002 to 0.003 in. in the proposed alloys. Results of the study of higher energy radiations that could be used with the modified Integral Method are shown in the following section.

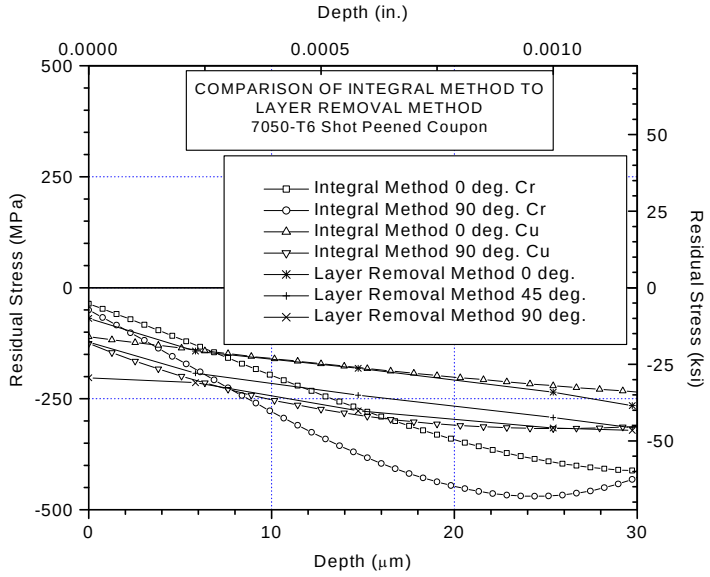

FIGURE 1. Comparison of integral method and layer removal methods on the compressive surface of shot peened 7050-T6 aluminum using both Cr and Cu Kα radiations.

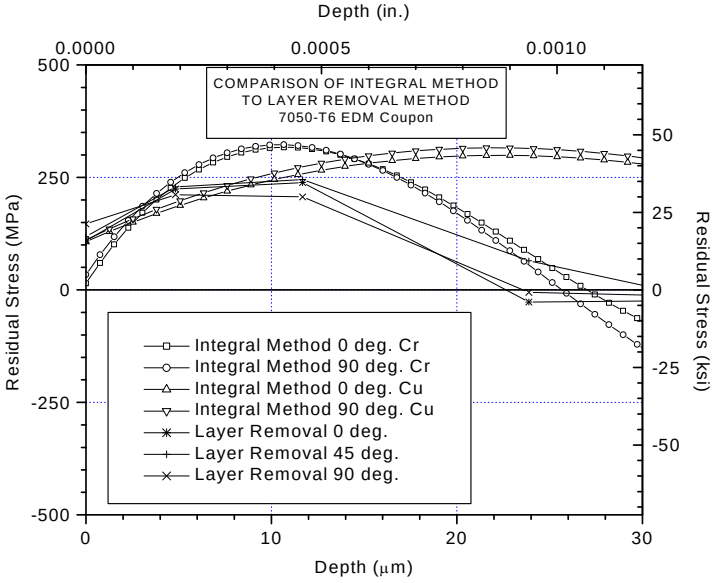

FIGURE 2. Comparison of the integral and layer removal methods on the EDM'd, tensile stressed 7050-T6 coupon using Cr and Cu Kα radiations.

RESULTS AND DISCUSSION

Computation of Diffraction Patterns

Three alloys were chosen for this investigation – Ti-6Al-4V, Ti-6Al-2Sn-4Zr-6Mo and IN100. Diffraction patterns were theoretically predicted for each alloy since they could not be empirically determined for most of the higher energy radiations of interest. The relative intensity of the diffraction lines are governed by the Powder Pattern Power theorem. The equation for the intensity of the powder pattern lines on a diffractometer is:[13]

$$I = |F|^2 p\left(\frac{1+\cos^2 2\theta}{\sin^2\theta\cos\theta}\right)e^{-2M} \quad (3)$$

Where I = the relative integrated intensity, F = structure factor, p = multiplicity factor, θ = Bragg Angle, and e^{-2M} is the temperature factor. The trigonometric term $(1+\cos^2 2\theta / \sin^2\theta\cos\theta)$ is the Lorentz-polarization factor.

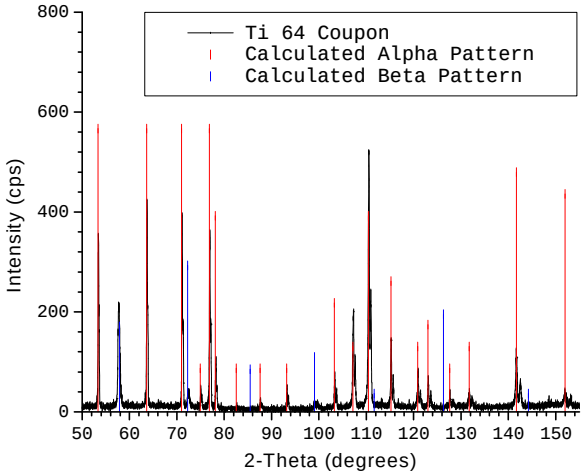

FIGURE 3. Measured and predicted diffraction pattern for Ti-6Al-4V with Cu Kα radiation showing good agreement between the two patterns.

Of the factors contributing to the relative intensity, the structure factor term dominates and is typically hundreds of times larger than the other terms. Since the structure factor decreases quickly as the Bragg angle increases, the higher order peaks produced with higher energy radiation will have very low intensity. This is observed in all the diffraction patterns shown, both theoretical and empirical, for the higher energy radiations. In addition the background intensity does not decrease at the higher angles therefore producing diminishing peak to background ratios. Continually decreasing peak intensity for the higher order peaks in combination with the high error in strain measurement at the lower Bragg angles, discussed in detail below, significantly limits the maximum radiation energy level that can be used.

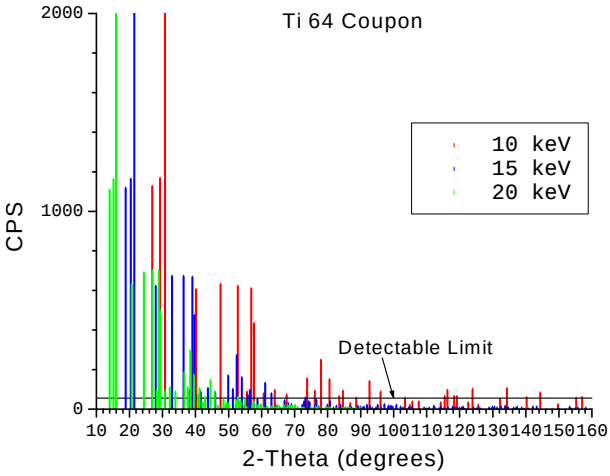

FIGURE 4. Computed diffraction patterns with 10, 15 and 20 keV radiations for Ti-6-4 showing detectable peaks at high Bragg angles for the 10 keV radiation.

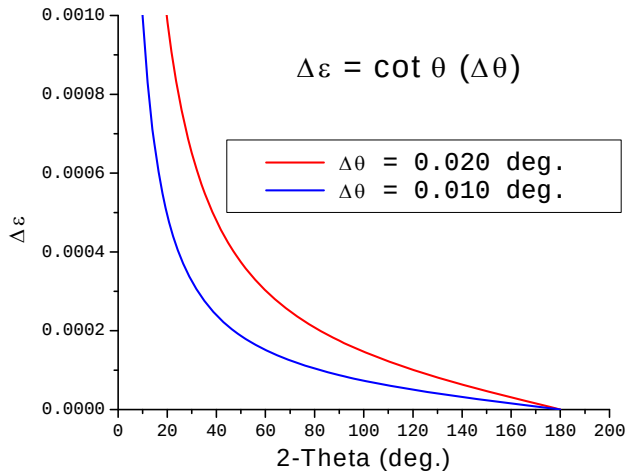

FIGURE 5. Error in strain vs. Bragg angle for a 0.01 and 0.02 deg. error in fitted peak position showing exponentially increasing error at low Bragg angles.

In order to theoretically determine what diffraction peaks were available for the proposed integral method it was first necessary to empirically

determine the lattice parameters for each alloy. A diffraction pattern was obtained for each alloy using Cu Kα radiation. The precise lattice parameters, a_0 and/or c_0, were calculated from the individual lattice spacings determined from the peaks from a diffraction pattern for each alloy. The position of the $K\alpha_1$ line was determined by peak profile analysis, fitting Pearson VII functions to separate the K-alpha doublet. The individual lattice spacings, d, were calculated from the Kα wavelength after correction for instrumental error. Detectable peaks were defined as those with an intensity of at least four times the empirical background and a Bragg angle position of at least 120 deg. or higher due to increased measurement error and diffracted beam cutoff at lower angles.

Diffraction patterns were computed for CuKα radiation and compared to the measured pattern for all three alloys. A comparison of the computed and measured diffraction patterns for CuKα are shown in Figure 3. The red and blue lines represent the computed peak position for the α and β phases, respectively. The predicted peak position and intensity for all materials were in reasonable agreement with empirical results. Any differences in peak intensity could be attributed to texture or grain size effects of the material.

Diffraction patterns were both measured and computed for higher energy MoKα radiation to demonstrate theoretical patterns were adequately predicting the peak positions and intensities for an x-ray energy higher than CuKα. All patterns showed good agreement between the calculated and measured results indicating that patterns can be predicted theoretically with acceptable accuracy for higher energy radiations.

Diffraction patterns were computed for higher energy radiations of 10, 15 and 20 keV for all three alloys. Computed patterns for Ti-6Al-4V are shown in Figure 6. The patterns for 10, 15 and 20 keV energies are shown in red, blue and green, respectively. The horizontal line near the X-axis represents the detectable diffraction peak limit of four-times the background intensity. Peak intensities decrease as the radiation energy and Bragg angle increase as predicted by the Powder Pattern Power theorem.

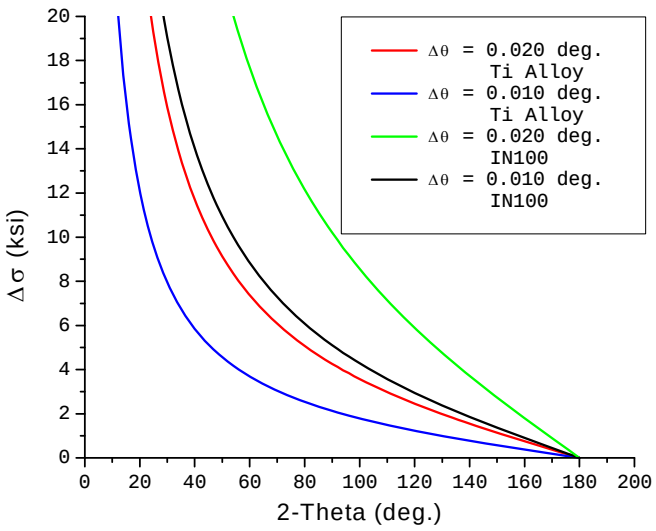

FIGURE 6. Error in measured residual stress vs. Bragg angle for 0.01 and 0.02 deg. error in fitted peak position for Ti alloys.

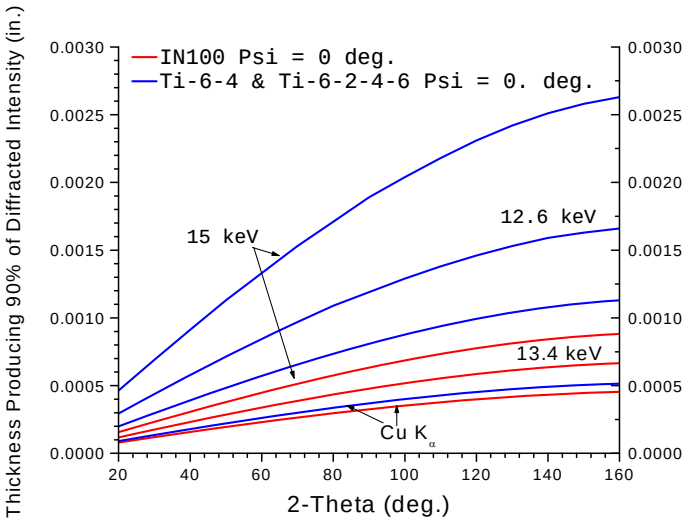

FIGURE 7. Depth of penetration vs. Bragg Angle for IN100.

Detectable peaks are available for stress measurement at relatively high Bragg angles with a radiation energy of 10 keV. However, at 15 and 20 keV the higher intensity peaks shift to Bragg angles of 70 deg. or less. At such low angles the peaks are not useful for residual stress

measurements due to a high error in strain measurement as shown in the next section.

Diffraction patterns were computed for energies at finer increments between 10 and 15 keV to determine more precisely the highest energy that resulted in a detectable peak at relatively high Bragg angles. Peak intensities above the detectable limit are produced, at high Bragg angles, at energies of 12.6 keV or less for both Ti alloys. The calculated patterns for IN100 indicate detectable peaks exist in the high-back reflection region for radiation energies as high as 13.4 keV.

Theoretical Determination of Measurement Error

The error in strain resulting from an error in the fitted peak position of 0.010 and 0.020 deg. was theoretically determined for the three alloys. The equation relating the error in measured strain to the error in peak position, shown in Equation 4, can be derived from Braggs Law.

$$\delta\varepsilon = \frac{\partial d}{d} = \cot\theta(\delta\theta) \qquad (4)$$

As shown in Equation 4 the error in measured strain is a function of the error in diffraction peak position and the cotangent of the Bragg angle. The cotangent term will increase to infinity as the Bragg angle approaches 0 deg. This significantly limits the use of low angle peaks for stress measurement.

The theoretical determination of error in strain resulting from an error in mean peak position of 0.010 and 0.020 deg. is shown in Figure 5 for all Bragg angles. For a given error in peak position the error in strain exponentially increases at the lower Bragg angles. The data reveal that the peak or peaks chosen should be at high Bragg angle to minimize error.

The error in stress measurement was computed from the error in strains for Bragg angles ranging from 0 to 180 deg. The stress errors were computed assuming a 0 to 45 deg. psi tilt using Equation 5, shown below.

$$\delta\sigma_{\phi} = \frac{E}{(1+\nu)\sin^2\psi}\left(\frac{\delta d}{d}\right) \qquad (5)$$

Where $E/(1+\nu)$ is the material's x-ray elastic constants.

Errors in calculated stress, resulting from an error in peak position, are shown in Figure 6. As in the case of the strains, the stress errors exponentially increase at lower Bragg angles. For an error in peak position of 0.020 deg. a diffraction peak should be chosen at a nominal position of 80 deg. or higher for the Ti alloys and at 130 deg. or higher for the IN100 in order to maintain an error in residual stress of ±5 ksi or lower

Determine Radiation Penetration Depths

X-ray penetration depths were computed for several radiation energies. Penetrations were computed for psi tilts of both 0 and 45 deg. The penetration depth was taken to be the thickness of material producing 90% of the diffracted intensity.

X-ray penetration depths for several radiation energies, at a psi tilt of 0 deg., are shown in Figure 7. Ti-6-4 and Ti-6-2-4-6 alloys produce almost identical depths of penetration and therefore are presented as the same curves. The penetration depth at an energy of 13.4 keV is nominally 40% deeper than CuKα radiation for IN100. Results indicate a potential 3X increase in penetration depth with 12.6 keV radiation energy over the currently used CuKα radiation for the Ti alloys.

Determination of Practical Radiations

Means of producing the higher energy radiations were considered. X-ray tube targets, white radiation, and synchrotron sources were evaluated. Practicality of each technique was based on such parameters as cost, equipment size, flexibility, and ease of integration with existing equipment and software; and influence on measurement error.

Elements that produce characteristic radiation between 12 and 14 keV are not practical for a radiation source. Elements emitting Kα and the lower intensity Lα characteristic radiation lines between 12 and 14 keV are impractical for various reasons including being non-metals, having very low melting points, or being radioactive.

Another method of obtaining the higher energy deeper penetrating radiation is through the use of the continuous radiation spectrum or white radiation. A readily available x-ray tube target such as Cu or Mo will produce a continuous spectrum of radiation containing different energies. Using a fixed Bragg angle, a Si(Li) detector, and a multi-channel analyzer

(MCA), the change in energy for a set of planes or a group of planes can be measured for various psi tilts to determine the residual stress.

Residual stress techniques using white radiation have been attempted and published.[11, 14-16] Compared to the conventional method (single wavelength, moving detector), energy dispersive diffraction is faster because the entire diffraction peak or peaks are determined simultaneously. However, the method suffers from poor accuracy for several reasons:

1. The resolution at which semiconductor counters can detect a shift in energy is inferior to that of the conventional method of measuring the angular shift in peak position.
2. The intensity of white radiation is much less than that of the characteristic Kα radiation.
3. White radiation measurements are usually made at relatively small Bragg angles in order to maximize the diffracted intensity.
4. As discussed previously, measurement error increases exponentially at lower Bragg angles.

Residual stress measurements have been made using a synchrotron source.[16-18] The advantage of the synchrotron source is it can provide a large range of radiation energies. The synchrotron source can also be used as a white radiation source. The radiation intensities of a synchrotron source are typically higher than conventional sources. The drawback however, is that synchrotron sources are very expensive and relatively large. Synchrotron sources are typically used in government or university facilities for research purposes. The relatively large size of the equipment will be a disadvantage if residual stress measurements are desired on-site or in the field.

CONCLUSIONS

- Several factors severely limit any appreciable increases in x-ray penetration depths over and beyond those currently used for IN100, Ti-6-4 and Ti-6-2-4-6 alloys.

- The error in strain measurement increases exponentially with lower Bragg angles restricting any use of lower order higher intensity peaks. Bragg angles of 80 deg. or higher for the Ti alloys, and 130 deg. or higher for the IN100, are necessary to maintain measurement errors of nominally ±5 ksi or less.

- At higher radiation energies the higher order peak intensities dramatically decrease as a result of the structure factor in the Powder Pattern Power theorem. This significantly limits the maximum energy that can be used while still providing reasonable peak intensity. Peak intensities are not acceptable for measurement at radiation energies providing adequate penetration depths.

- A practical radiation source that would produce the higher energies found to provide acceptable peaks in the high Bragg angles is not available. Elements for x-ray tube targets emitting the higher energy radiations are not practical. White radiation methods are not viable due to low intensity and low measurement resolution. Synchrotron sources provide adequate intensity however, are too expensive and large for a practical measurement device.

- A non-destructive x-ray diffraction method of measuring to depths of 0.002 to 0.003 in. in IN100, Ti-6-4 and Ti-6-2-4-6 does not appear to be feasible with the current technology.

REFERENCES

1. Sasaki, T. and Kuramoto, M., (1984), "X-ray Multiaxial Stress Analysis Taking Account of Stress Gradient," Adv. in X-Ray Analysis, 27, Plenum Press, New York, NY, pp. 121-128.
2. Noyan, I.C. and Cohen, J.B., (1984), "Determining Stresses in the Presence of Nonlinearities in Interplanar Spacing vs. $Sin^2(\psi)$," Adv. in X-Ray Analysis, 27, Plenum Press, New York, NY, pp. 129-148.
3. Predecki, P. K., Zhu, X. and Ballard, B., (1993), "Proposed Methods for Depth Profiling of Residual Stresses Using Grazing Incidence X-Ray Diffraction (GIXD)," Adv. in X-Ray Analysis, 36, Plenum Press, New York, NY, pp. 237-245.
4. Shibano, J., Tadano, S., and Ukai, T., (1996), "Polychromatic X-Ray Method for Residual-stress Measurements in a Subsurface Layer," *Exp. Mech.*, **36**[1], pp. 24-32.
5. Pfeiffer, W. and Hollstein, T., (1993), "Damage Determination and Strength Prediction of

Machined Ceramics by X-Ray Diffraction Techniques," NIST Special Publication 847, pp. 235-11.
6. Hollstein, T. Pfeiffer, W., et al, (1996), "Analysis of Machining Damage in Engineering Ceramics by Fracture Mechanics, Fractography and X-ray Diffraction," Fractography of Glasses and Ceramics III, American Ceramic Society, Westerville, OH, pp. 145-169.
7. Pfeiffer, W., (1992), "Characterization of Near-Surface Conditions of Machined Ceramics by Use of X-ray Residual Stress Measurements," Residual Stresses-III: Science and Technology, Vol. 1, Elsevier Applied Science, New York, NY, pp. 607-612.
8. Eigenmann, B., Scholtes, B. and Macherauch, E., (1989), "Determination of Residual Stresses in Ceramics and Ceramic-Metallic Composites by X-ray Diffraction Methods," *Material Science and Engineering*, **A118**, pp. 1-17.
9. Wern, H. and Suominen, L., (1996), "Self Consistent Evaluation of Non-Uniform Stress Profiles and X-ray Elastic Constants From X-ray Diffraction Experiments," Adv. in X-Ray Analysis, 39.
10. Wern, H., (1995), "Finite-Element Solutions for Mechanical Drilling Methods: A New Integral Formalism," *J. of Computing. and Appl. Math.*, 63, pp. 365-372.
11. Shibana J., et al, (1994), "Measurement Method of the Stress Distribution Along a Depth by Polychromatic X-ray," Advances in X-Ray Analysis, 207-213.
12. Prevey, P and Hornbach, D, (1988), "X-ray Measurements and Residual Stresses in Ground/Polished Ceramics," NIST Final Report, NIST SBIR (Contract 50-DKNB-7-90128), January.
13. Cullity, B.D., (1956), Elements of X-ray Diffraction, Addison-Wesley Publishing Company, Inc., Reading, MA, ed. M. Cohen.
14. Black, D.R., Bechtoldt, C.J., Placious, R.C. and Kuriyama, M., (1985), "Three Dimensional Strain Measurements with X-Ray Energy Dispersive Spectroscopy," Journal of Nondestructive Evaluation, 5(1), 21-25.
15. Genzel C., Stock C., Wallis B, and Reimers W., (2001), "The Application of White Radiation to Residual Stress Analysis in the Intermediate Zone Between Surface and Volume," 467, 1253-1256, Part 2 July 21.
16. Pyzalla A., (2000), Methods and Feasibility of Residual Stress Analysis by High-Energy Synchrotron Radiation in Transmission Geometry Using a White Beam", 19: (1) 21-31 March.
17. Barral M., Sprauel, Jean-Mechel, Lebrun, Jean-Lou, (1986), "On The Use of Synchrotron Radiation For the Study of The Mechanical Behaviour of Materials," 149-158.
18. Kuntz T. et. al., (1993) "Residual Strain Gradient Determination in Metal-Matrix Composites by Synchrotron X-Ray-Energy Dispersive Diffraction," Met Transactions A-Physical Metallurgy and Materials Science, 24: (5) 1117-1124, May.